

COMPUTATIONAL ANALYSIS OF PENTAMODE STRUCTURES UNDER COMPRESSIVE LOADING

PANAGIOTIS N. LYMPEROPOULOS EFSTATHIOS E. THEOTOKOGLOU AND
KONSTANTINOS KALFOUNTZOS

* Department of Mechanics, Laboratory of Testing and Materials, School of Applied Mathematical and Physical Sciences, National Technical University of Athens, 5, Heroes of Polytechnion Avenue, Theocaris Building Zografou Campus, PO Box 157 73 Athens, Greece
e-mail: panagiotislymperopoulos@mail.ntua.gr, stathis@central.ntua.gr

Key words: Metamaterials, pentamode structure, computational mechanics, finite element method, compressive loading, buckling.

Summary. Pentamodes mechanical metamaterials are lattice structures that are applied in many engineering applications. Buckling of pentamodes lattice structures is a phenomenon that may be occurred when high compressive loadings are considered. Due to the lattice structure of pentamodes, buckling analysis may be a complicated phenomenon. In our study, a numerical investigation of pentamodes under compressive loading conditions has taken place. Several pentamodes structures have been analyzed. Von Misses stresses have been calculated and maximum stresses are determined. Finally, a buckling analyses considering material non linearity has also taken place.

1 INTRODUCTION

Buckling is a significant nonlinear deformation that can occur to beams under high compressive loading. Pentamodes mechanical metamaterials are lattice structures, composed of bi-cone beams and are designed to have high bulk modulus [1-3]. They can confront different high compressive loading conditions and consequently buckling phenomena may occur. In addition, due to the non-homogeneous nature of pentamodes, the response of pentamodes under different loading conditions is significantly affected. Their wide applications field, from aerospace structure to vibrations isolation structure (antiseismic design) [2,4,5]] contribute to further investigation of buckling characteristic of pentamode structures.

In addition, pentamodes with increased height have also been used in order to confront different loading conditions [5-10]. For this reason, buckling analyses should be taken place, in order to analyse the buckling characteristics of pentamodes structures.

The present paper deals with the buckling response of pentamodes structures. More specifically, the main objective of this study is the investigation of failure mechanism of pentamodes structures under high compressive forces, which results buckling phenomena, using the Finite Element Method (FEM). The aforementioned procedure is implemented using FEM package ANSYS [11] which incorporates nonlinear FEM analyses and buckling

analysis. The elastoplastic material behaviour of Clear V4 polymer [10] is modelled using a bilinear stress-strain relationship. In addition, large displacement analyses have taken place. The convergence of the numerical solution is also tested for different pentamode structures.

Load displacement curves have been created using the results from the FEM analyses. In addition, Von Misseses stresses contours have been developed to determine the maximum stress fields and their amplitude taking into consideration material and geometric non linearity. It is also found that pentamodes appear to rotate under compressive loading, due to their non-homogenous nature.

2 THEORETICAL CONSIDERATION

2.1 Pentamode structure

In our study, a typical pentamode unit cell (Figure 1) is used,

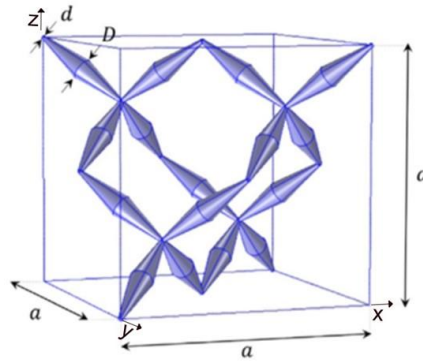


Figure 1: Unit cell pentamode structure [4,5]

where d is the small diameter, D is the wide diameter and a is the main dimension of pentamode structure. In Table 1, the dimensions of pentamodes are presented.

Table 1: Pentamoded dimensions

α [mm]	d [mm]	D [mm]
30	2.4	5.4

The pentamodes structures considered in this study have unit cells towards x-axis (n_x) and respectively for y- and z-axis (n_y, n_z), as presented in Table 2.

Table 2: Pentamoded Structures

Case	Unit Cell
1	$n_x = n_y = 2, n_z = 1$
3	$n_x = n_y = 6, n_z = 1$
5	$n_x = n_y = 10, n_z = 1$

2.2 Materials

In our analyses, pentamodes are considered to be made from the polymer resin Clear V4 [12]. The materials stress strain curves are given in Figure 2.

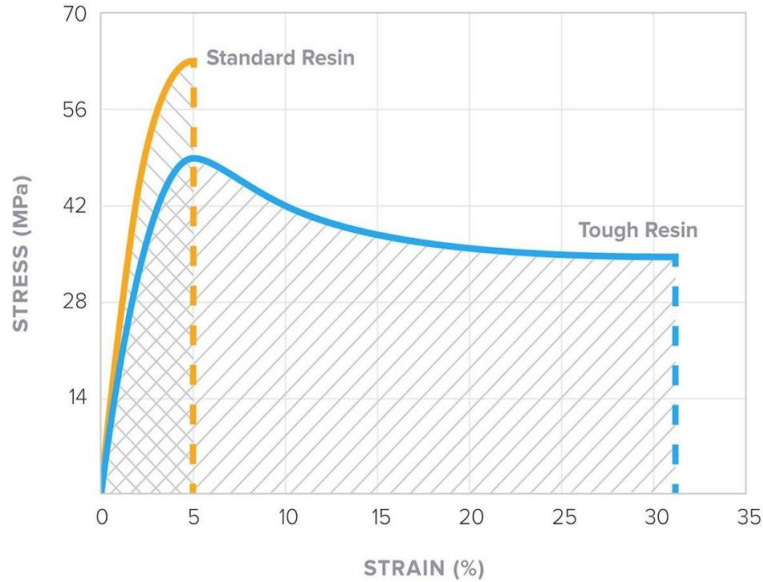


Figure 2: Material properties [12]

From Figure 2, Clear V4 [12] is considered to be the standard resin that has been used in our analyses. The Young modulus of the material is 2.8[GPa], the ultimate tensile strength is 65[MPa] while the elongation at failure is 6% [12].

3 COMPUTATIONAL ANALYSIS

In this finite element analyses, pentamodes have been modeled using the finite element program ANSYS[11]. The element that has been used is the BEAM189 [11] which is a 3 nodes beam element, with 6 degrees of freedom each node. In order to confront the beam bicone geometry, TAPER [11] elements have also been used. At first in order to study the convergence of our results, a pentamode with $D=5mm$, $d=1.4mm$, $\alpha=30mm$ and with $n_x = n_y = n_z = 2$ is considered. A compressive load of 1.5kN is applied to nodes at the upper side of the pentamodes, whereas the nodes at the bottom side are fully constrained. The displacements of the upper side of the pentamodes is plotted in the following Figure 3.

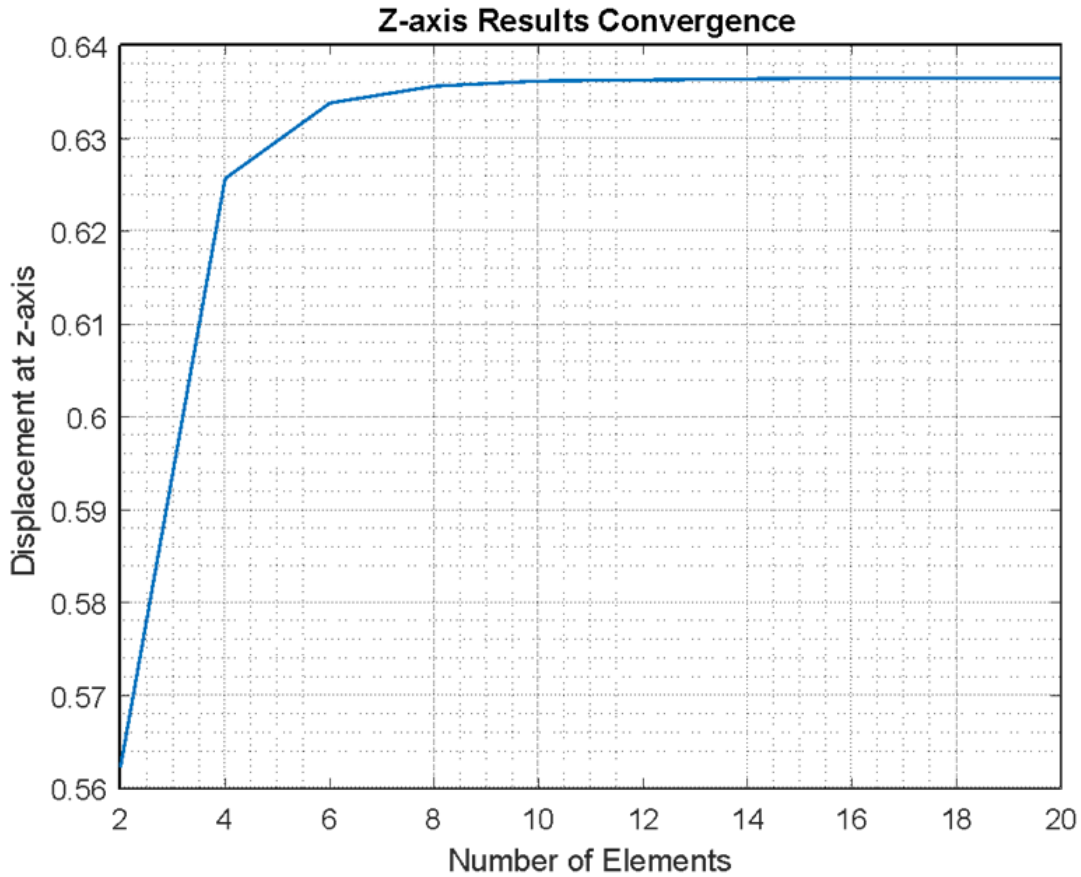


Figure 3: Convergence of the displacement

In Figure 3, the results for the displacements of the upper side nodes are presented. It is observed that the results convergence after 16 elements in each beam. In our study 20 elements in each beam are considered.

The buckling finite element analyses is divided in two parts. At the first part, a static finite element analyses is take place, with a compressive load of 1N. Then, with the results from the static analyses, an eigenbuckling analyses is considered. The eigenbuckling analyses extract 3 eigenfrequencies each case.

4 RESULTS AND DISCUSSION

In this section, the results of the finite element analyses are presented. In our study two cases for the boundary conditions are considered. At first, pentamodes bottom side nodes are considered fully constrained, and secondly the bottom side nodes are considered to have only the displacements constrained. Then the eigenvalue forces are calculated, and for the first eigenvalue each case, the Von Misses stresses are extracted.

3.1 Eigenvalue Forces

For the 1st case, the eigenvalue forces are given in the Table 3,

Table 3: Eigenvalue forces

Eigenvalue force	Fully Constrained [N]	Only Displacements Constrained [N]
1 st	156.38	133.38
2 nd	452.86	444.33
3 rd	653.73	653.20

According to Table 3, it is observed that the 1st eigenvalue force in the case of the fully constrained bottom side nodes has higher value than in the case of only displacements constrained at the bottom side nodes. It should be noted that the 1st eigenvalue force is the most useful during the design process.

For the 2nd case, the eigenvalue forces are presented in the Table 4,

Table 4: Eigenvalue forces

Eigenvalue force	Fully Constrained [N]	Only Displacements Constrained [N]
1 st	67.12	65.80
2 nd	566.00	555.06
3 rd	718.79	718.17

As it is also noted from the results of Table 4, the 1st eigenvalue force in the case of fully constrained bottom side nodes has higher value than in the case of only displacements constrained at the bottom side nodes.

Finally for the 3rd case, the eigenvalue forces are given in Table 5,

Table 5: Eigenvalue forces

Eigenvalue force	Fully Constrained [N]	Only Displacements Constrained [N]
1 st	42.14	41.72
2 nd	371.42	367.90
3 rd	566.42	565.96

From the results of Table 5, it is also observed that the 1st eigenvalue force for the case of fully constrained bottom side nodes has higher value than the case of only displacements constrained at the bottom side nodes.

In the sequel, for the case of $n_x = n_y = 6$ and $n_z = 1$, a comparison of the 1st eigenvalue force among different beams dimensions has taken place (Table 6).

Table 6: Pentamoded dimensions

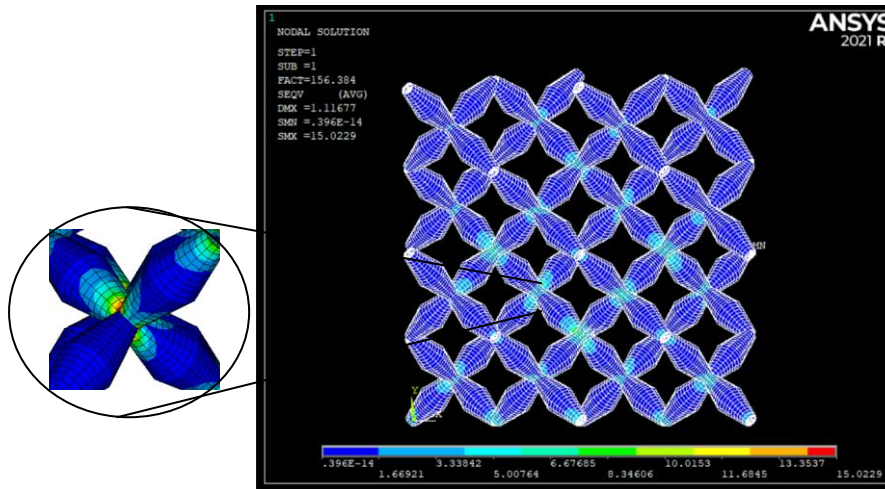
	d [mm]	D [mm]	Eigenvalue force [N]
1	4.8	10.8	907.16
2	1.2	5.7	4.43

It is observed that pentamode with wider beam dimensions present higher eigenvalue force

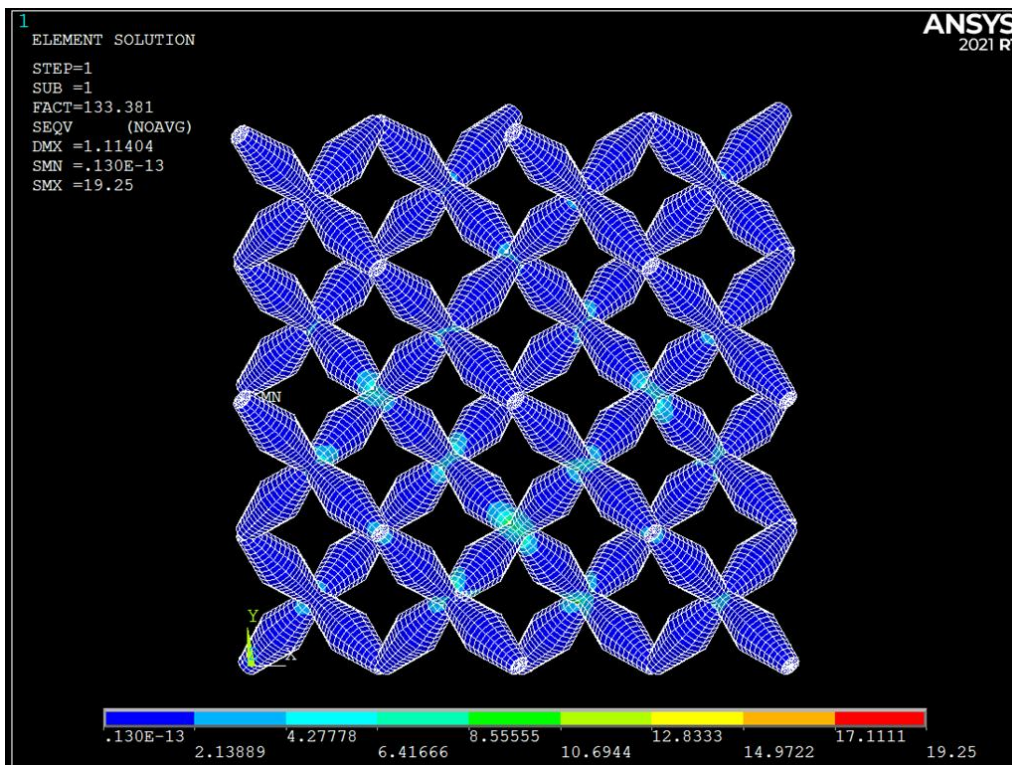
than that with the pentamode with thinner beam dimensions.

3.2 Von Misses Stress

In order to determine where the maximum stresses will be appeared, the Von Misses stresses are calculated. For the 1st case (Table 3), and for both boundary conditions, the Von Misses stresses are given in Figure 4.



(a) Fully constrained bottom side nodes

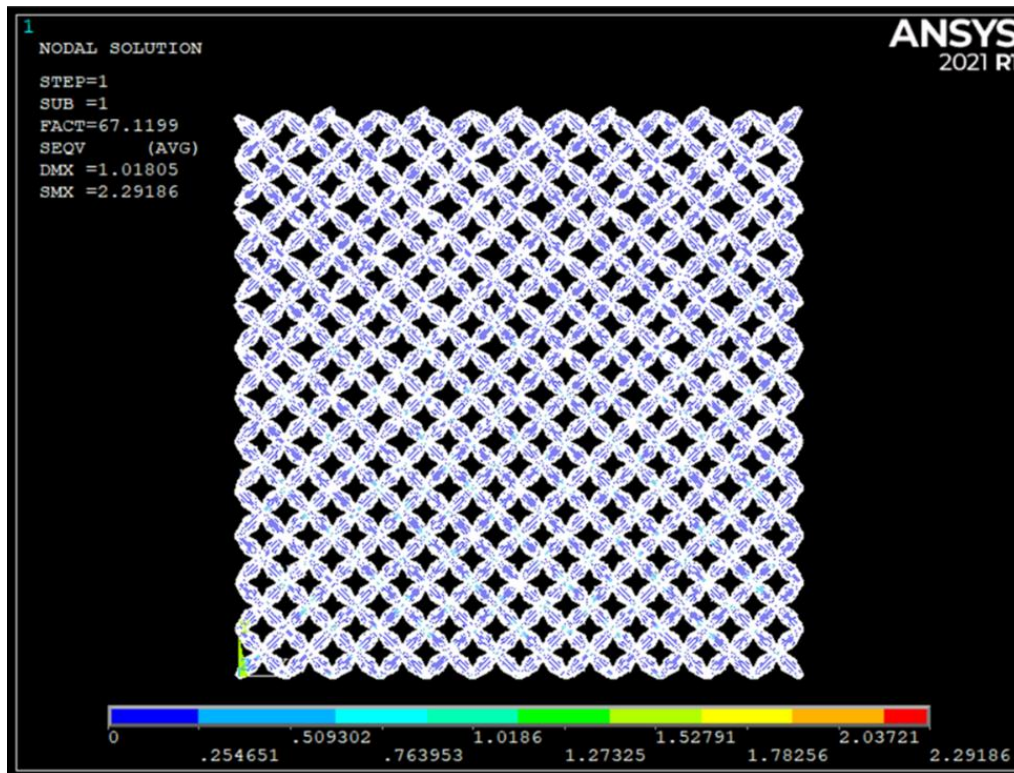


(b) Only displacements constrained bottom side nodes

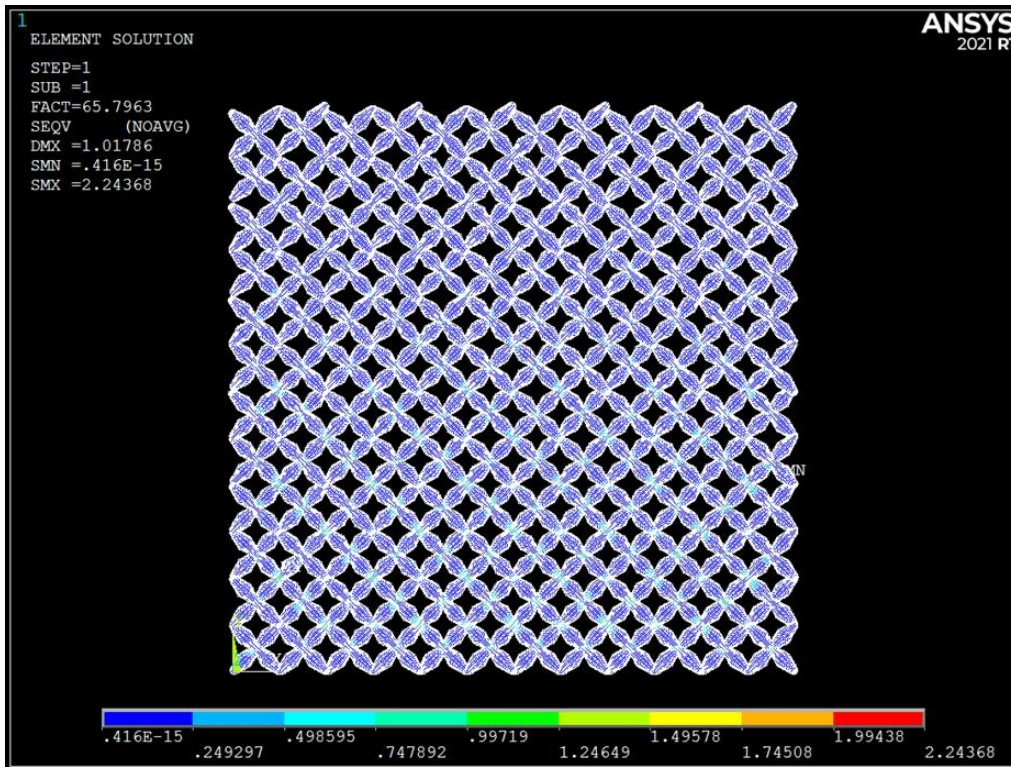
Figure 4: Von Misses stress in the 1st case (Table 3)

It is observed that the maximum Von Misses stresses, are near the beam connections. The maximum Von Misses stresses are between 15.02[MPa] and 19.25[MPa] for both cases respectively, which is below the ultimate strength of the material (Section 2.2).

In the sequel for the 2nd case (Table 4), and for both boundary conditions, the Von Misses are presented in Figure 5.



(a) Fully constrained bottom side nodes

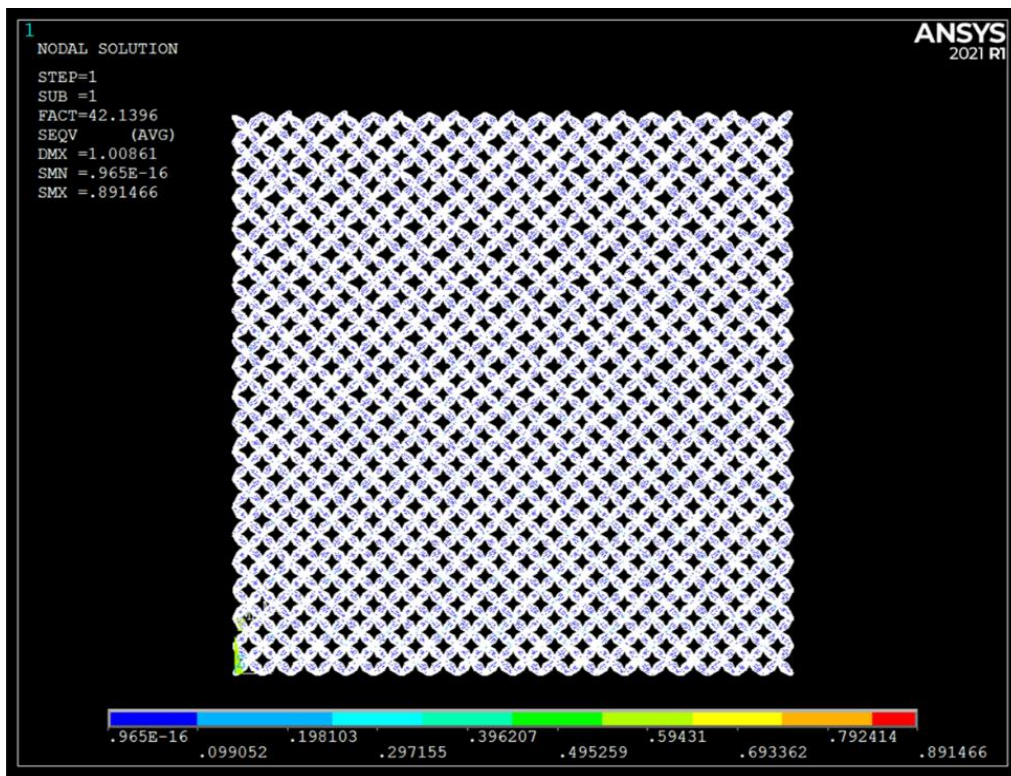


(b) Only displacements constrained bottom side nodes

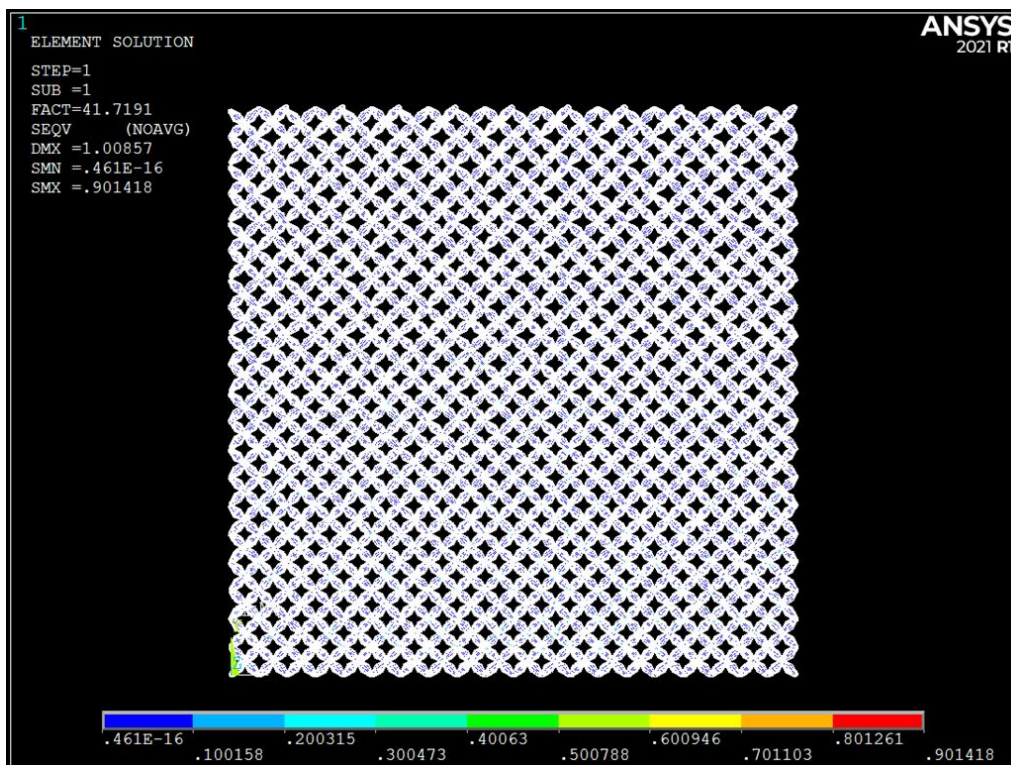
Figure 5: Von Misses stress in the 2nd case (Table 4)

From Figure 5 it is should be noted that the maximum Von Misses stresses, are near beam connections. In addition, according to Figures 4, 5, the maximum Von Misses stresses appeared lower value in the 2nd case than in the 1st case. The maximum Von Misses stresses are between 2.29[MPa] and 2.24[MPa] for both cases respectively, which is below the ultimate strength of the material (Section 2.2).

For the 3rd case (Table 5), and for both boundary conditions, the Von Misses are given in Figure 6.



(a) Fully constrained bottom side nodes



(b) Only displacements constrained bottom side nodes

Figure 6: Von Misses stress in the 3rd case (Table 5)

From Figure 6 it also is observed that the maximum Von Misses stresses are between 0.89[MPa] and 0.90[MPa] for both cases respectively, which is below the ultimate strength of the material (Section 2.2).

3.3 Non linear buckling

For the case of $n_x = n_y = 6$ and $n_z = 1$, a non linear buckling analyses has taken place. The material is considered to be bi-linear (Figure 2), and the corresponding eigenvalue forces are presented in the Table 7.

Table 7: Eigenvalue forces

Eigenvalue force	Fully Constrained [N]
1 st	67.12
2 nd	566.00
3 rd	718.79

It is observed from Tables 5 and 9 that the eigenvalue forces almost coincide for the linear and non linear buckling analyses.

4 CONCLUSIONS

In this study, a buckling analyses of pentamodes has taken place. Linear buckling characteristics were considered for several pentamodes structures under different boundary conditions. According to our study, pentamodes with fully constrained bottom side nodes, appeared higher 1st eigenvalue force than pentamodes with only displacements constrained at the bottom side nodes. In addition, Von Misses stresses appeared to have decreased maximum values in the case of pentamodes only displacements constrained at the bottom side nodes. Furthermore, as pentamodes increased their dimensions, the 1st eigenvalue force appeared to decrease. In addition, the non linear buckling analyses presented results for the eigenvalue forces that almost coincided with those from the linear analyses.

Finally, for future work, large displacement analyses should take place in more materials options. Furthermore, a new fillet type for the beam connections [13] should also be considered.

REFERENCES

- [1] Fleck, A. N., Deshpande, S. V., Ashby, F. M. Micro-architected materials: past, present and future. Proceedings of the Royal Society of London A. 2010;466; 2495–2516
- [2] Kadic M., Bueckmann T., Stenger N., Thiel M., Wegener M., On the practicability of pentamode mechanical metamaterials, Applied Physics Letters, 2012, 100, p.p. (191901-1)-(191901-4).
- [3] Norris N. A., Mechanics of elastic networks. Proceedings of the Royal Society of London

- A, 2014, 470 (2172).
- [4] F. Fabbrocino, A. Amendola, F. Benzoni and F. Fraternali, Seismic Application of Pentamode Lattices, *International Journal of Earthquake Engineering*, 2015, 62-71.
- [5] Amendola A , Carpentieri G , Feo L , Fraternali F . Bending dominated response of layered mechanical metamaterials alternating pentamode lattices and confinement plates, *Composite structures*, 2016, 157, 71–77.
- [6] Zhang L, Song B., Zha A., Liu R., Yang L., Shi Y., Study on mechanical properties of honeycomb pentamode structures fabricates by laser additive manufacturing: Numerical and experimental verification, *Composite Structures*, 2019 226, 111199.
- [7] Lin G., Li J., Chen P., Sun W., Chizhik S. A., Makhaniok A. A., Melnikova G. B., Kuznetsova T. A., Buckling of lattice columns made from three-dimensional chiral mechanical metamaterials, *International Journal of Mechanical Sciences*, 2021, 194, 105208.
- [8] Wang Y., Chi Z., Liu J., On buckling behaviors of a typical bending-dominated periodic lattice, *Composite Structures*, 2021, 258, 113204.
- [9] Cushing C. W., Kelsten M. J., Su X., Wilson P. S., Haberman M. R., Norris A. N., Design and characterization of a three-dimensional anisotropic additively manufactured pentamode material, *The Journal of the Acoustical Society of America*, 2022, 151, p.p. 168–79
- [10] Lympopoulos P. N., Theotokoglou E. E., Numerical Investigation of Pentamode Mechanical Metamaterials, *WSEAS Transactions on Applied and Theoretical Mechanics*, 2022, vol. 17, pp. 47-55.
- [11] ANSYS, ANSYS mechanical user' s guide (Release 19.0): Pennsylvania, USA: ANSYS Inc. 2018.
- [12] FormLabs. Standard Materials for High-Resolution Rapid Prototyping, 2017, 1–3.
- [13] M. Dallagoa, S. Raghavendraa, V. Luchinb, G. Zappinib, D. Pasinic, M. Benedettia, The role of node fillet, unit-cell size and strut orientation on the fatigue strength of Ti-6Al-4V lattice materials additively manufactured via laser powder bed fusion. *Int. J. Fatigue* 2021, 142, 105946.